

# Synthesis and Characterization of Nanocrystalline $\text{La}_{0.65}\text{Sr}_{0.3}\text{MnO}_3$ and $\text{La}_{0.8}\text{Sr}_{0.2}\text{MnO}_3$ Cathode Powders by Auto-ignition Technique for Solid Oxide Fuel Cells (SOFC)

G.N. Almutairi\*, M. Ghouse, Y. M. Alyousef, and F.S. Alenazey

Water and Energy Research Institute (WERI), King Abdulaziz City for Science and Technology (KACST)  
PO.Box.6086, Riyadh 11442, Saudi Arabia

Received: April 17, 2016, Accepted: June 15, 2016, Available online: June 28, 2016

**Abstract:** Solid Oxide fuel Cells (SOFCs) are considered to be one of the most promising energy conversion devices that have several advantages such as high efficiency, system compactness and low environmental pollution. In the present investigation  $\text{La}_{0.65}\text{Sr}_{0.3}\text{MnO}_3$  (LSM-1) and  $\text{La}_{0.8}\text{Sr}_{0.2}\text{MnO}_3$  (LSM-2) nanoceramic powders were prepared by citrate-nitrate route of auto-combustion with citrate to nitrate (c/n) ratio 0.50 to see the effect of these cathode powders on the performance of SOFC cells. The as prepared powder were calcined at  $900^\circ\text{C}$  for 4hrs using the Thermolyne 47900 furnace to remove carbonaceous residues and characterized them using SEM / EDS, XRD, TGA techniques and their results are presented. From calculations using Debye Scherrer's equation, the average crystallite size of the powders were found to be around 16nm. The SEM indicates the particle sizes are within the range of around 200nm. The surface area of the calcined LSM-2 powder was found to be  $\sim 21\text{m}^2/\text{g}$ . The TGA studies indicate the completion of combustion since there was no further weight loss after reaching temperature of  $\sim 650^\circ\text{C}$ .

Also, Electrochemical characterization of LSM cathode powders were carried out by coating these powders (as cathode functional layer CFL-Bottom and current collector layer CL- Top) using Screen printing on the SOFC half cells (NiO-YSZ+YSZ) procured from CGCRI, Kolkata, India with a cell size of 16mm dia x 1.6mm and tested these cells with  $\text{H}_2\text{-O}_2$  at  $750\text{-}800^\circ\text{C}$  with the flow rates of 100-200 sccm. The results of the performances of single cells are presented in this paper. The Current density and powder density values obtained are  $0.80\text{A}/\text{cm}^2$  (at 0.7V) and  $0.55\text{W}/\text{cm}^2$  at  $800^\circ\text{C}$  with 200 sccm of hydrogen and oxygen respectively. The area surface resistance (ASR) values obtained were  $\sim 0.50\ \Omega\text{cm}^2$  at 0.7V at  $800^\circ\text{C}$ .

**Keywords:** LSM, SOFC, NiO-YSZ, TGA, SEM, CFL, CL

## 1. INTRODUCTION

The clean, efficient and sustainable energy has stimulated great interest in the fuel cells. Among all types of fuel cells, solid oxide fuel cells (SOFC) offer the highest energy efficiency and the greatest fuel flexibility such as hydrocarbons fuels, bio-derived renewable fuels [1-3]. The Solid oxide fuel cells (SOFCs) are one of the prominent candidates of power generators that convert chemical energy directly and with high efficiency, into electricity while causing little pollution [4,5]. However, the commercialization of SOFC technology is hindered due to high cost involvement. For economically viable system, better materials have to be developed to meet the challenges. The  $\text{La}_{0.8}\text{Sr}_{0.2}\text{MnO}_3$  (LSM) is known to be a classical cathode material for SOFC based yttria-stabilized Zir-

conia electrolyte because of its high electrical conductivity, excellent thermal, chemical stability and compatibility with  $\text{ZrO}_2$  based electrolyte at the working temperatures  $800\text{-}1000^\circ\text{C}$ . The cathode for  $\text{O}_2$  reduction is an important area for SOFC development since its performance is often dominated by cathode polarization mainly at lower operating temperatures where inexpensive materials may be used for the components of SOFC. There are several methods used to produce LSM powders such as solid phase synthesis, sol-gel and electrochemical synthesis methods prepared [6-9]. Ze Liu et al [10] studied LSM-infiltrated LSCF cathodes for anode supported solid oxide fuel cells at  $825^\circ\text{C}$ . Obtained a power density of  $\sim 1.07\text{W}/\text{cm}^2$  and about 24% higher power output than without LSM infiltration and there was little degradation in cell performance over a period of 100hrs. The current status of the development of a SOFC cell unit is based on yttria-stabilized zirconia (YSZ) solid electrolyte and electrodes consist-

\*To whom correspondence should be addressed: Email: gmotari@kacst.edu.sa  
Phone: Tel:+966 11 4813061, Fax: +966 11 4813880  
<http://www.kacst.edu.sa>

ing of Sr-doped  $\text{LaMnO}_3$  (Cathode) and Ni-YSZ cermet (Anode) [11,12]. Although LSM is an excellent cathode material for high temperature SOFC due to its good stability, high catalytic activity toward oxygen reduction and excellent compatibility with YSZ electrolyte, it becomes less efficient when the cell operating temperature is reduced due to its low electronic and ionic conductivity, leading to a drastic decrease in active sites beyond the three-phase-boundary [13-14]. In spite of significant efforts have been put until now by various researchers, fundamental questions on the mechanism and kinetics of the  $\text{O}_2$  reduction reaction and on the electrode behavior of LSM materials under fuel-cell operation conditions still remain unsolved.

In recent years it was attempted to use  $\text{La}_{0.65}\text{Sr}_{0.3}\text{MnO}_3$  with 50% YSZ as a cathode function layer to enhance the cell performance [15,16]. Pal et al [15] have prepared  $\text{La}_{0.65}\text{Sr}_{0.3}\text{MnO}_3$  with L-alanine to nitrate ratio of 1:1 using auto-ignition process and studied their thermal and electrical and electrochemical properties at 600-800°C. Haanappel et al [16] studied the optimization of processing and microstructural parameters of LSM cathodes to improve the performance of anode supported SOFCs. They have studied the effect of cathode functional layer varying various ratios of LSM : YSZ with calcined and un-calcined YSZ powders. They concluded that the un-ground LSM for cathode current collector layer and non-calcined YSZ powder for the cathode functional layer (CFL) simplifies the production of SOFC fuel cell. The current density values obtained are  $1.5\text{A}/\text{cm}^2$  at 0.7V with LSM:YSZ ratio of 50:50 by wt % at 800°C. Buchkremer et al [17] reported with a double layered  $\text{La}_{0.65}\text{Sr}_{0.3}\text{MnO}_3$  (LSM) / LSM - $\text{Y}_2\text{O}_3$ - stabilized  $\text{ZrO}_2$  (YSZ) cathode applied on a thin YSZ and operated between 800-1000°C. The current density achieved was  $0.5\text{A}/\text{cm}^2$  at 750°C at 0.7V.

In the present investigation it is attempted to study the effect of combination of  $\text{La}_{0.8}\text{Sr}_{0.2}\text{MnO}_3$  and  $\text{La}_{0.65}\text{Sr}_{0.3}\text{MnO}_3$  cathode powders on the performance of the SOFC cells. The CFL (50wt%  $\text{La}_{0.65}\text{Sr}_{0.3}\text{MnO}_3$  -50wt%YSZ) as cathode functional layer and CL ( $\text{La}_{0.8}\text{Sr}_{0.2}\text{MnO}_3$ ) as current collector layer were used. The nanocrystalline LSM powders were prepared by auto-ignition technique since it is a simple and more economical way of making nano ceramic powders and studied their physical and electrochemical characteristics at 700-800°C using  $\text{H}_2$  and  $\text{O}_2$  in a specially designed and fabricated fuel cell test station and collected the data to draw I-V and I-P curves.

## 2. EXPERIMENTAL PROCEDURE

### 2.1. Preparation of $\text{La}_{0.65}\text{Sr}_{0.3}\text{MnO}_3$ (LSM-1) and $\text{La}_{0.8}\text{Sr}_{0.2}\text{MnO}_3$ (LSM-2) nanoceramic powders

The  $\text{La}_{0.65}\text{Sr}_{0.3}\text{MnO}_3$  (LSM-1) and  $\text{La}_{0.8}\text{Sr}_{0.2}\text{MnO}_3$  (LSM-2) nano ceramic powders were prepared by auto-combustion technique [18-

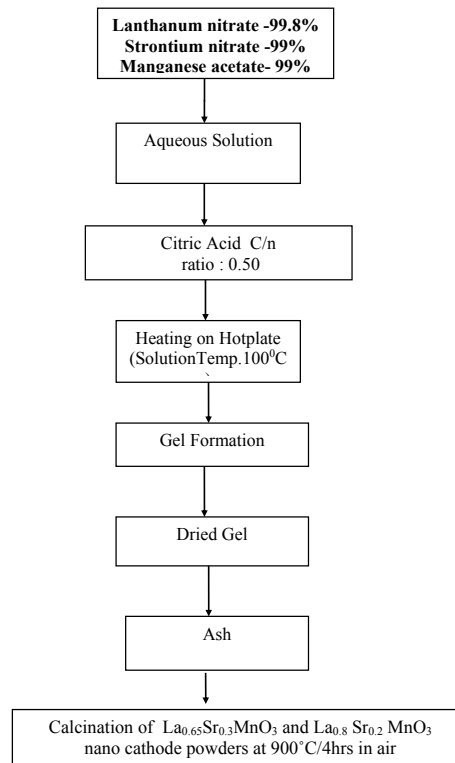


Figure 1. Flow Chart for preparing of  $\text{La}_{0.65}\text{Sr}_{0.3}\text{MnO}_3$  (LSM-1) and  $\text{La}_{0.8}\text{Sr}_{0.2}\text{MnO}_3$  (LSM-2) cathode nano ceramic powders by Auto-ignition Technique [ 18-20]

20] using appropriate required amounts of  $\text{La}(\text{NO}_3)_3 \cdot 6\text{H}_2\text{O}$  (BDH),  $\text{Sr}(\text{NO}_3)_2$ , and  $\text{Mn}(\text{CH}_3\text{COO})_2 \cdot 4\text{H}_2\text{O}$ , citric acid (BDH) and distilled water. The precursor solution was prepared by mixing individual aqueous solution with the above chemicals with 99.0% purity. Then required citric acid was added to the all nitrate solutions mixed properly until to get clear solution without any precipitation in to the pyrex glass. The citrate / nitrate ratio maintained was 0.50. The pyrex glass beaker with the solution was heated to evaporate on a hot plate at 250°C using magnetic stirrer until a chocolate colored gel was formed. When the heating was continued further, the gel gets completely burnt on its own and becomes light, and fragile ash is obtained. Then the ash was calcined at 900°C/4hrs in a Barnstead Thermolyne 47900 Furnace (USA). Fig. 1 shows the flow Sheet for the preparation of LSM Powders by auto-ignition technique. Table 1 shows LSM powder samples prepared and Table 2 shows the physical properties of yttrium stabilized zirconium oxide (YSZ) powder [21].

Table 1. Batches of cathode LSM nano ceramic powders prepared by auto-ignition technique

LSM-1 Cathode Sample ID 242a, 242b	Cathode Functional Layer (CFL)	LSM -2 Cathode current collector Layer (CL) Sample ID # 201a, 201b
-	50% LSM-1 + 50% YSZ [Inter Layer]	-
$\text{La}_{0.65}\text{Sr}_{0.35}\text{MnO}_3$ C/N: 0.50		$\text{La}_{0.8}\text{Sr}_{0.2}\text{MnO}_3$ C/N: 0.50 [Top Layer over CFL]

a: as prepared, b: calcined at 900°C/4hrs

Table 2 Properties of Tosoh Yttrium Stabilized Zirconia powder -YSZ [21]

S.no	Physical Characteristics	Value
1	Crystallite size nm	25
2	Particle size D50 $\mu\text{m}$	0.6
3	Granule size D50 $\mu\text{m}$	60
4	Bulk density $\text{g}/\text{cm}^3$	1.3
5	Surface area $\text{m}^2/\text{gr}$	16
6	Loss of ignition (1000°C) wt%	1.5

CL (3 layers) 30 - 40 microns	The CFL and CL coatings were applied by Screen printing technique (d)
CFL (1 layer ) 10-15 microns	
YSZ- 12-15 microns	These SOFC Half Cells were procured from CGCRI (c)
Half Cell NiO-YSZ 1.5 mm thick	

Figure 2. Scheme of SOFC single cell assembly-16mm dia Cells (NiO-YSZ-YSZ + CFL+CL)

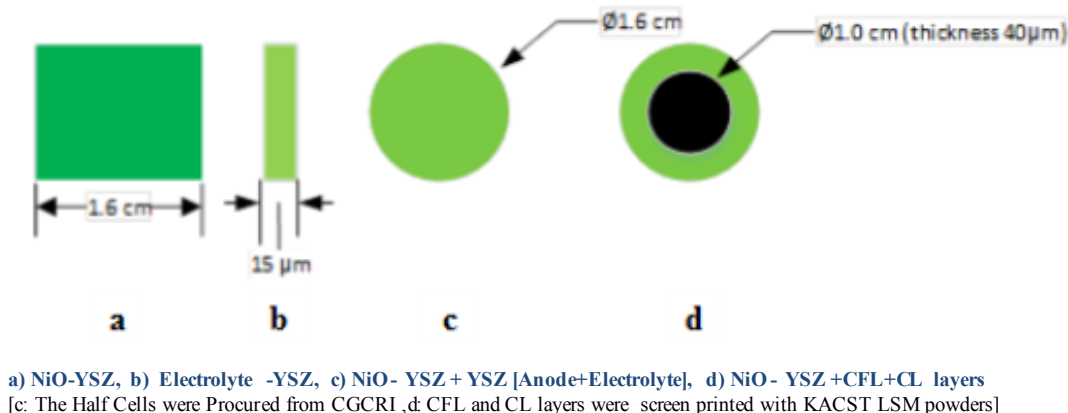


Figure 3. Single cell components – cathode screen printed cells (of 1mm dia with CFL and CL)

## 2.2. SEM / EDS Characterization

Small amounts of the samples were spread on adhesive conductive aluminum tapes attached to sample holders, coated with thin films of gold and examined by the Scanning Electron Microscope. The equipment used for analysis was JEOL-JSM-6010Plus / LV Scanning Electron Microscope, Japan. Equipped with an energy dispersive X-ray Analyzer (EDX) analysis system. Scanning Electron Microscope operated at 20KV. The energy dispersive X-ray Analyzer (EDX) was used to determine the elemental compositions and their distribution at area and spot on polished cross section of the full fuel cells. Imaging was performed in Secondary Electron (SEI) mode only using an accelerating voltage of 20keV.

## 2.3. XRD Characterization

(a) A part of the samples were analyzed by X-Ray Diffractometry (XRD) System. The crystalline phases of the samples were examined by X-ray diffraction analysis MiniFlex; Rigaku, Japan for phase characterization. The X-ray Diffractometry with  $CuK\alpha$  radiation at 40KV and 35mA was used for phase analysis with in a diffraction angle 2 theta range 10-70° and particle size determination from X-ray line broadening technique using the following Debye Scherrer Equation [22]:

$$t = 0.9\lambda / B \cos \theta$$

where  $t$  = Average crystallite size in nm,  $\lambda$  = the wave length (0.15418nm) of Cu  $K\alpha$  radiation,  $B$  the width (in radian) of the XRD diffraction peak at half of its maximum intensity (FWHM) , and  $\theta$  the Bragg diffraction angle of the line, and  $B$  is the line

width at half peak intensity.

(b) For comparison to find approximate average particle size, the following equation was used:

$$D_{BET} : 6 / (S_{BET} \times d_{th}) [23]$$

where  $D_{BET}$  is the average particle size in nm ,  $S_{BET}$  Surface area in  $m^2/g$  and  $d_{th}$  is the theoretical density of the material in  $gr/cc$ . [assuming that the particles have spherical shape and uniform size]

## 2.4. Surface Area Characterization

The surface area of samples was measured using Autosorb-1C instrument manufactured by Quanta Chrome , USA. Samples were taken in the range of 0.1 - 0.2 g in a cell and were degassed at 300°C for 3 hrs to remove any absorbed material on the surface. Nitrogen gas was used as adsorbent. The surface area ( $m^2/g$ ) of the as prepared powder and after calcined powder at 900°C have been calculated.

## 2.5. TGA Characterization

In order to determine the decomposition behavior of the LSM samples, around 7-8mg of the samples were loaded in a alumina crucible and put inside the thermo balance of TG Machine ( Perkin-Elmer Thermal Analysis) . The thermal decomposition behavior was studied up to 800°C The Half Cells of SOFC with 16mm dia and 1.5mm thick with NiO-YSZ 1.5mm thick and YSZ that was raised at a rate of  $\sim 10^\circ C$  per minute. The Thermal Gravimetric Analysis (TGA) of LSM-1 and LSM-2 powder plots are presented.

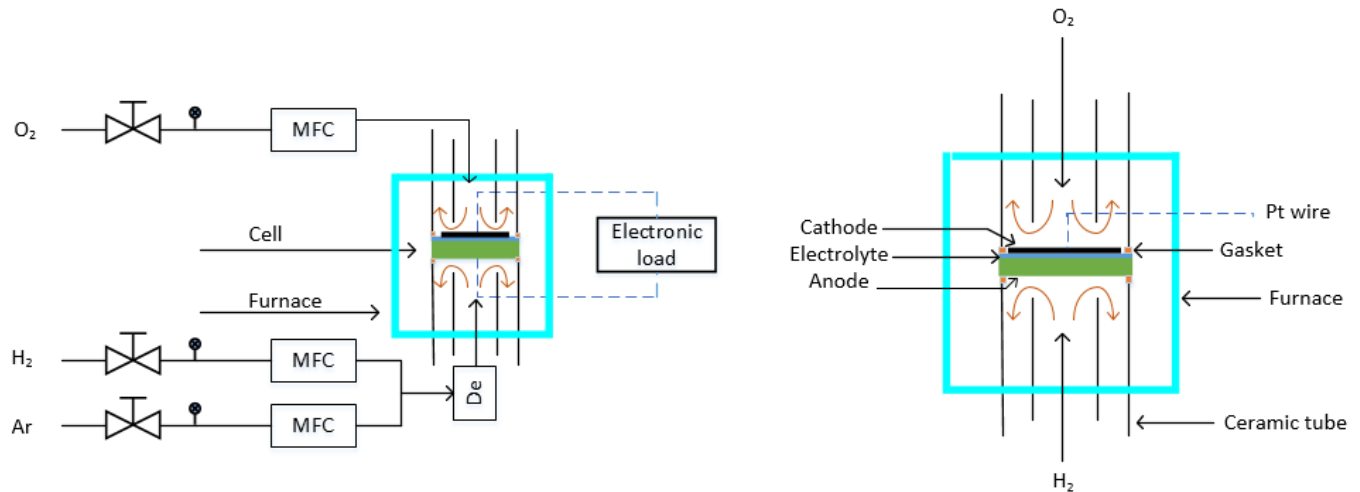


Figure 4. a Schematic of Experimental Set-up to test 16mm dia SOFC Single Cells [ 26, 27]



Figure 4. b Experimental Set-up for testing 16mm dia single SOFC cells

1.Furnace with anode and cathode compartments, 2.Humidifier, 3 Furnace Temperature controller, 4. Electronic Load Bank, 5. AgilentMultimeter,, 6. MKS Flow meters (H<sub>2</sub>, O<sub>2</sub>, Ar gases), 7. Platinum mesh - current collectors.



Figure 4. c Close view of Experimental Set-up with anode and cathode compartments and Single SOFC cell assembly at the center

references [24, 25].

## 2.6. Electrochemical Characterization

### 2.6.1. SOFC Half Cells (16mm dia x 1.5mm) Procured from CGCRI, Kolkata, India

The NiO-YSZ +YSZ half cells of 16mm dia x1.5mm thick were procured from CGCRI, Kolkata, India on commercial bases. The anode (NiO-YSZ) has thickness 1.5mm and electrolyte (YSZ) thickness was around 15 microns. These Half Cells (NiO-YSZ-YSZ) were Fabricated with Tape casting Technique to get anode (NiO-YSZ) and electrolyte (YSZ) layers and then laminated and pressed at room temperature and subsequently co-sintered both anode and electrolyte at 1400°C / 6 hrs at a rate 1°C/hr .The details of the electrode fabrication (half cells) process are described in the

### 2.6.2. Preparation cathode functional Layer (CFL) Paste (LSM-1 + 50% YSZ) and cathode catalyst Layer (CL) Paste (LSM-2)

The milled powders of CFL and CL were weight separately and prepared pastes to apply on half cells. The cleaned agate bowl and grinder were wiped with isopropyl alcohol / acetone with tissue paper. Taken 10 gr of cathode active layer ( cathode function layer-CFL) powder and 10gr catalyst powder LSM-2 were taken into two agates separately with 2 gr. of binder (ethyl cellulose) with 20-25 drops of thinner (terpinol) and mixed thoroughly for 2 hrs to get homogeneous paste. The thinner was added for every half an hour. The two pastes are collected in to two small bottles.

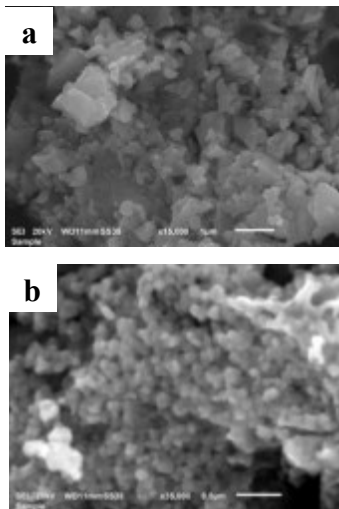


Figure 5. a. SEM of LSM-1 after calcination, b. SEM of  $La_{0.65}Sr_{0.3}MnO_3$  LSM-1 [After Milling for 24hrs]

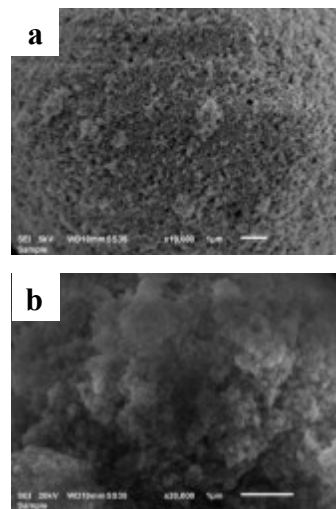


Figure 6. a. SEM of YSZ powder as received, b. SEM of YSZ powder after milled for 24hrs

### 2.6.3. Screen printing of the CFL and CL layers on the NiO-YSZ half Cells

The CFL layer ( 1 layer of 10-15microns ) was first printed over the YSZ surface of half cell then dried for 30minutes . Then 3 layers (~ 30 - 40 microns) of LSM-2 cathode paste successively over dried CFL layer using the Screen printer –SKYHILL Ming Tai Screen Printing Machine co Ltd, China . After drying of the screen printed half cells, they are taken in a dense alumina plate and put them in in the furnace covered with another plate and sintered them at 1050°C/ 4hrs at Room Temperature to 600°C (1 hr) at 75°C/h and then up to 1050°C at 100°C/hr then cool down at 150°C / hr to room Temperature. Now the full cell is ready for testing in a fuel cell test station.

### 2.6.4. Description of Experimental Set-up for testing 16mm dia SOFC Cells and assembly

The Test Station to evaluate single SOFC cells was procured from CGCRI (Central Glass Ceramic Research Institute), Kolkata, India. It is designed and fabricated by CGCRI. It is similar to the SOFC test stations and configurations reported by other researchers [26,27]. The brief description of the test station is given in the following paragraph:

It has vertical furnace with two compartments anode and cathode with alumina tubes with gas supply arrangements with MKS mass flow meters (type 247-4 channel readout) for argon, hydrogen and oxygen gases . The Agilent multimeter34401A and D.C.Electronic Load Bank are connected to the system to measure the cell voltage and current of the cell. Humidifier with glass balls around ~40 nos with 5mm dia and water of 50ml is fixed before entering hydrogen to the cell ( Figures 4a-4c). The Cell is loaded vertically . Hydrogen gas is passed from the bottom of the anode compartment and oxygen gas is passed from top of the cathode compartment the single cell of 16mm dia x 1.6mm thick is placed between to two Alumina tubes with current collector with platinum mesh of area 0.3cm<sup>2</sup>. So the effective electrode area is considered as 0.3cm<sup>2</sup>. The anode side

NiO-YSZ is faced toward hydrogen gas and CFL+CL screen printed over electrolyte of the halfcell faced towards oxygen gas. The cell is sealed using glass rings melting at 1000°C. Then the furnace temperature is brought down to 800°C with temperature controller M/S A.G.Enterprise West Bengal, India, Argon and hydrogen were purged in the anode chamber and simultaneously the voltage was recorded. The purging and simulations gas switching from argon to hydrogen and oxygen in the anode and cathode compartments were kept on till the voltage is reached to open circuit voltage (OCV) of 1.10V. The electrochemical performance was evaluated using variable flow rates of fuel – hydrogen and oxidant oxygen viz 100-200sccm respectively. The electrochemical performance were recorded in the temperature range of 700-800°C at an interval of 50°C and I-V and I-P curves are plotted with varying gas flow rates (100-200 sccm).

## 3. RESULTS AND DISCUSSION

### 3.1. Physical characterization

#### 3.1.1. SEM / EDX

Fig 5a and Fig 5b show the SEM images for LSM-1 powders. It is seen that the oxide particles are well crystallized with clear shape and the particle dia is less than 300nm [28]. It is clearly seen that the particle sizes of the above powders reduced after milling for 24 hrs under ethanol media with ZrO<sub>2</sub> balls of size 5mm dia.. These powders were milled and dried at 100°C for preparing CFL before applying on the half cells of 16mm dia . Fig 6a and Fig 6b show the as received YSZ powder and milled for 24hrs with ethanol for 24hrs respectively. It is clearly seen in the reduction in the YSZ particles. The properties of YSZ powders are given in Table 2. Fig 7a and Fig 7b show the CFL powder after milled for 24hrs using ZrO<sub>2</sub> balls of 5mm dia. It is seen fine structure with fine particles less than 200nm.

Fig 8a and Fig 8b show the SEM image of LSM-2 powders of calcined and milled for 24hrs respectively indicating the particle size reduction and the morphology of is characterized by sphere

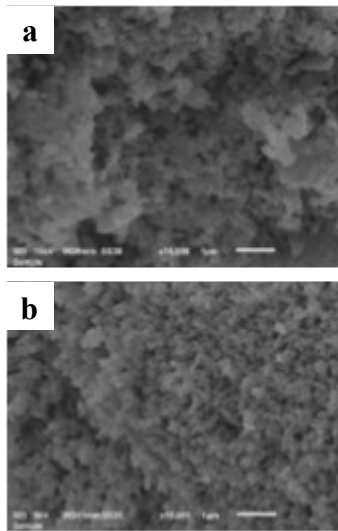


Figure 7. SEM of CFL-1(LSM-1+50%YSZ) Powder after milled for 24hrs

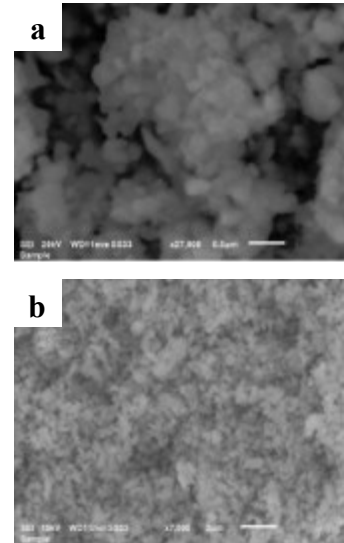


Figure 8. a SEM of LSM-2 Calcined at 900°C/4hrs, b SEM of LSM-2 calcined and milled powder

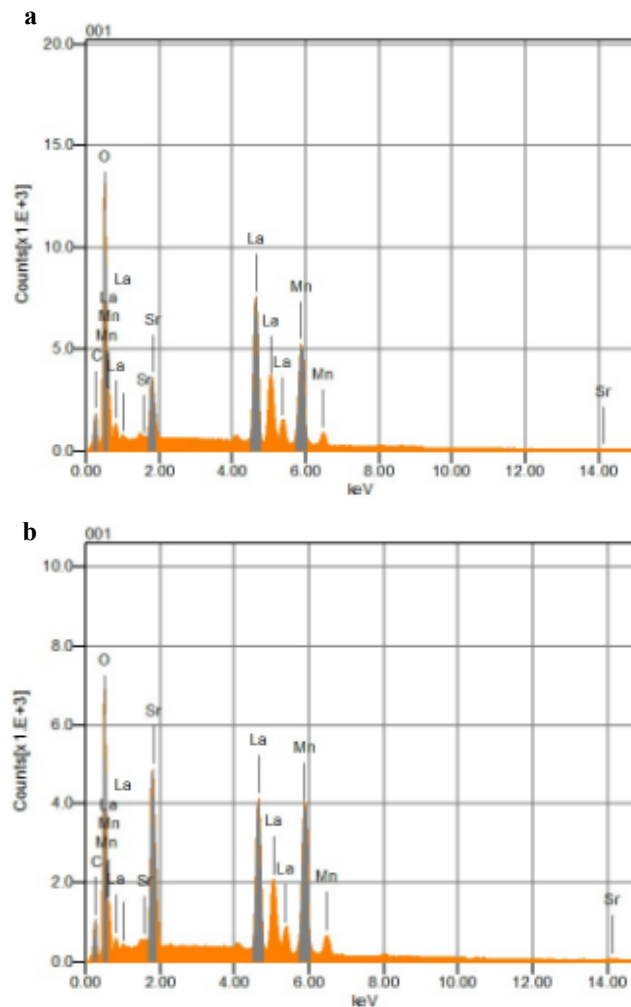


Figure 9. a EDS pattern of LSM-2 powder Calcined at 900°C/4hrs, b EDS pattern of LSM-1 calcined and milled-24hrs

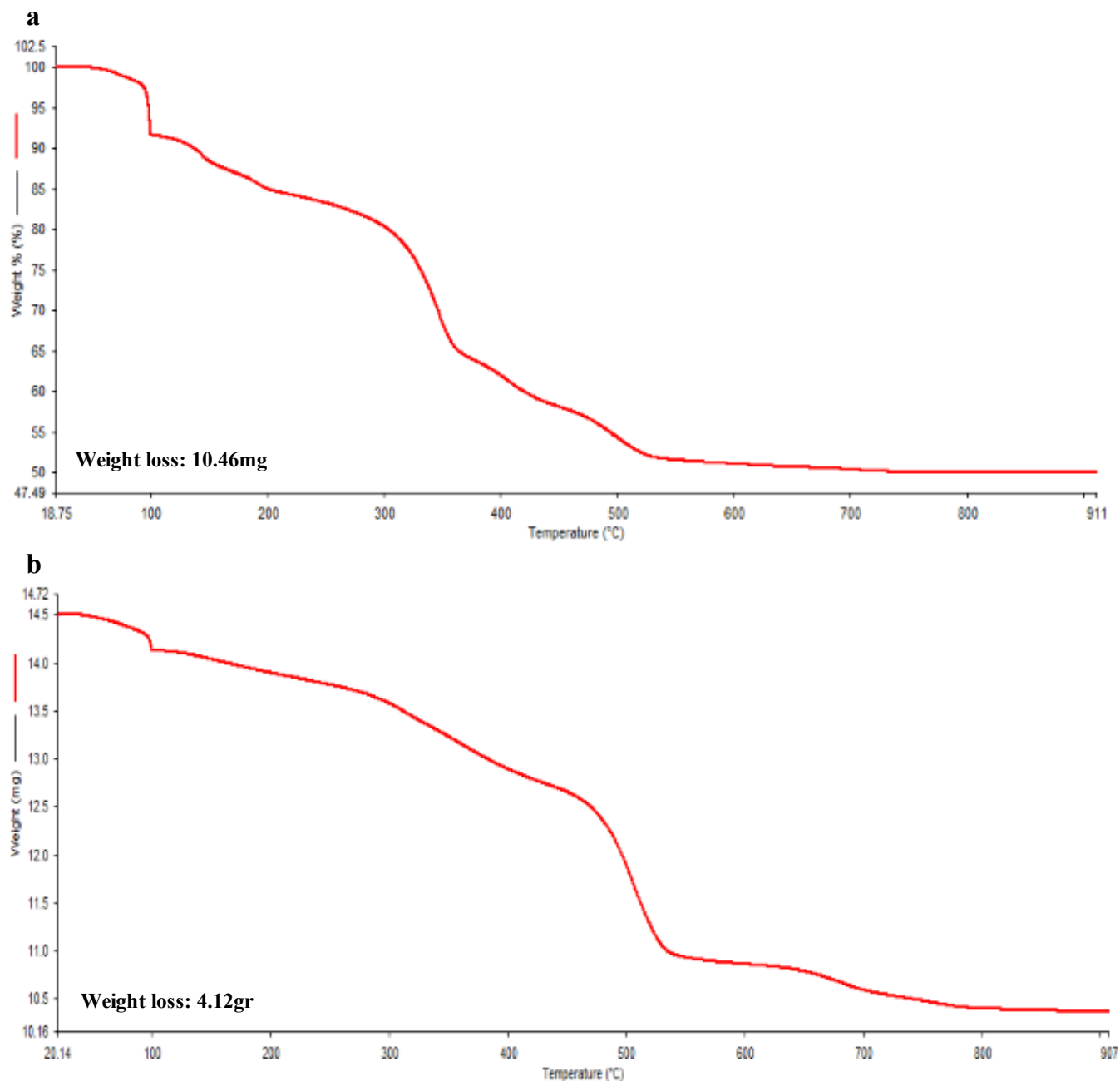


Figure 10. a TGA Plot of LSM -2 powder (As prepared) #201, b TGA Plot of LSM -1 Powder (As prepared) #242

Table 3. Results of EDS analysis

Component	Weight %					Weight %			Atomic %			Atomic ratio		
	La	Sr	Mn	C	O	La	Sr	Mn	La	Sr	Mn	La : Sr : Mn		
$La_{0.8}Sr_{0.2}MnO_3$ [Calcined]	41.91	7.44	18.04	9.30	23.31	62.19	11.04	26.77	45.77	12.59	48.72	0.94	0.25	1
$La_{0.65}Sr_{0.3}MnO_3$ [Calcined]	32.95	15.59	20.27	10.34	20.85	47.50	22.82	29.67	34.2	26.04	53.99	0.64	0.48	1

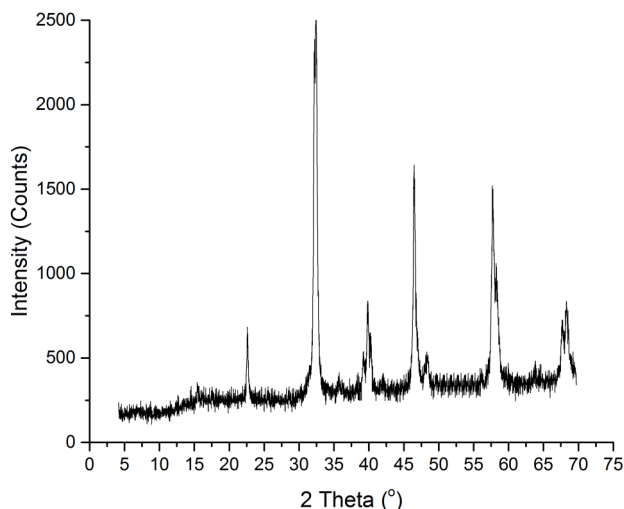


Figure 11. XRD patterns of  $\text{La}_{0.8} \text{Sr}_{0.2} \text{MnO}_3$  [LSM-2] cathode powder (calcined)

type particles (ranging around 200-300nm). with slight agglomeration Fig 9a-9b show the EDS plots of the LSM-2 and LSM-1 powders along with the qualitative amounts of elements present in the powders. According to the EDS analysis (Table 3 ) of LSM -2 and LSM-2 powders formed the components with slight variation in the atomic ratio.

### 3.2 TGA Characterization

Figures 10a and 10b show the thermal analysis of as prepared LSM nano powders in the range of 30-900°C. It is seen from the TGA plots of LSM-2 and LSM-1 that the drastic weight loss occurred at about 220°C for both the powders and weight loss found to be 10.46gr and 4.12g for as prepared LSM-2 and LSM-1 respectively. After an initial small weight loss of adsorbed water at 160°C, indicating decomposition of metal-citrate complexes and formation of crystalline phase of the LSM powders. No further weight loss is observed after reaching temperature of ~600-650°C in the TGA plots which indicates completion of combustion. The Thermal behavior of both the powders are found to be similar in nature. Similar trend is seen as reported elsewhere for LSM powders [ 29-31].

### 3.3. XRD characterization

Fig 11 show the XRD patterns of the  $\text{La}_{0.8} \text{Sr}_{0.2} \text{MnO}_3$  calcined powder at 900°C. It is seen that the peaks obtained are similar to the other authors reported [32,33]. It is seen that small amounts of  $\text{Mn}_3\text{O}_4$  is present which might come from the change of oxidation

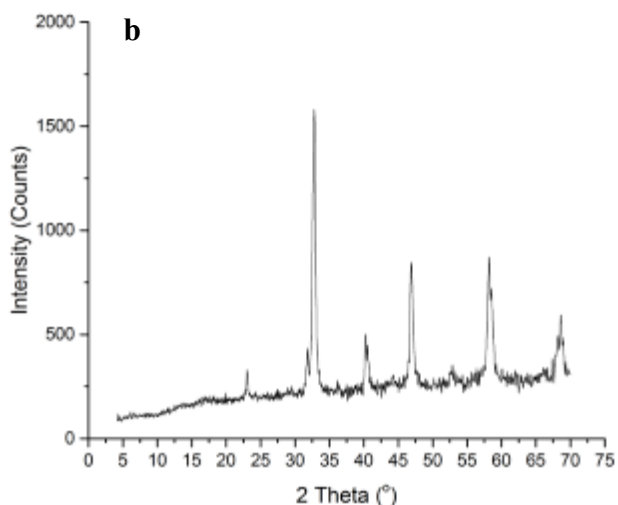
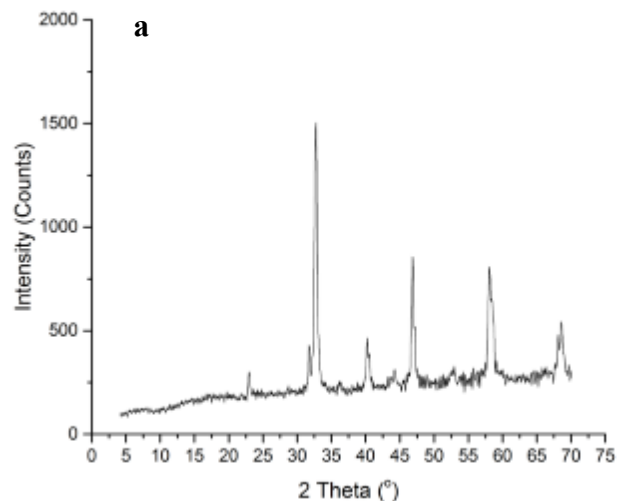


Figure 12. a XRD patterns of  $\text{La}_{0.65} \text{Sr}_{0.3} \text{MnO}_3$  (LSM-1) cathode powder (calcined), b XRD patterns of  $\text{La}_{0.65} \text{Sr}_{0.3} \text{MnO}_3$  (LSM-1) cathode powder calcined and milled

state of the Mn ion. The crystallite size of the LSM-2 powder was 15.2nm and LSM-1 powder was 14.99nm (Table 3). Fig 12a and b shows the XRD pattern of calcined  $\text{La}_{0.65} \text{Sr}_{0.2} \text{MnO}_3$  powder and milled powder respectively . The phase analysis of the diffractogram reveals that it consists of predominantly rhombohedral phase together with an orthorhombic phase. The powder obtained after calcination at 900°C was pure and it is quite comparable with the

Table 4. XRD Data to determine the average crystallite size of the LSM powders

Sample ID Number	With $\text{CuK}\alpha$ Radiation $\lambda (\text{Co}) = 0.15418\text{nm}$	
	B FWHM	Crystallite size, t (nm)
201a [LSM-2] (as prepared )	-	-
201b [LSM-2] (Calcined at 900°C / 4hrs)	0.5487	15.20
242a [LSM-1] (as prepared )	-	-
242b [LSM-1] (Calcined at 900°C / 4hrs)	0.5211	15.88
242b [LSM-1] (Calcined milled for 24 hrs)	0.5522	14.99

Average crystallite size =  $t = 0.9 \times \lambda / B \cos \theta$ ,  $B = \text{FHHM in } ^\circ$ ,  $B = [\text{FWHM} \times 22/7 + 180] = \text{FWHM} \times 0.017460$



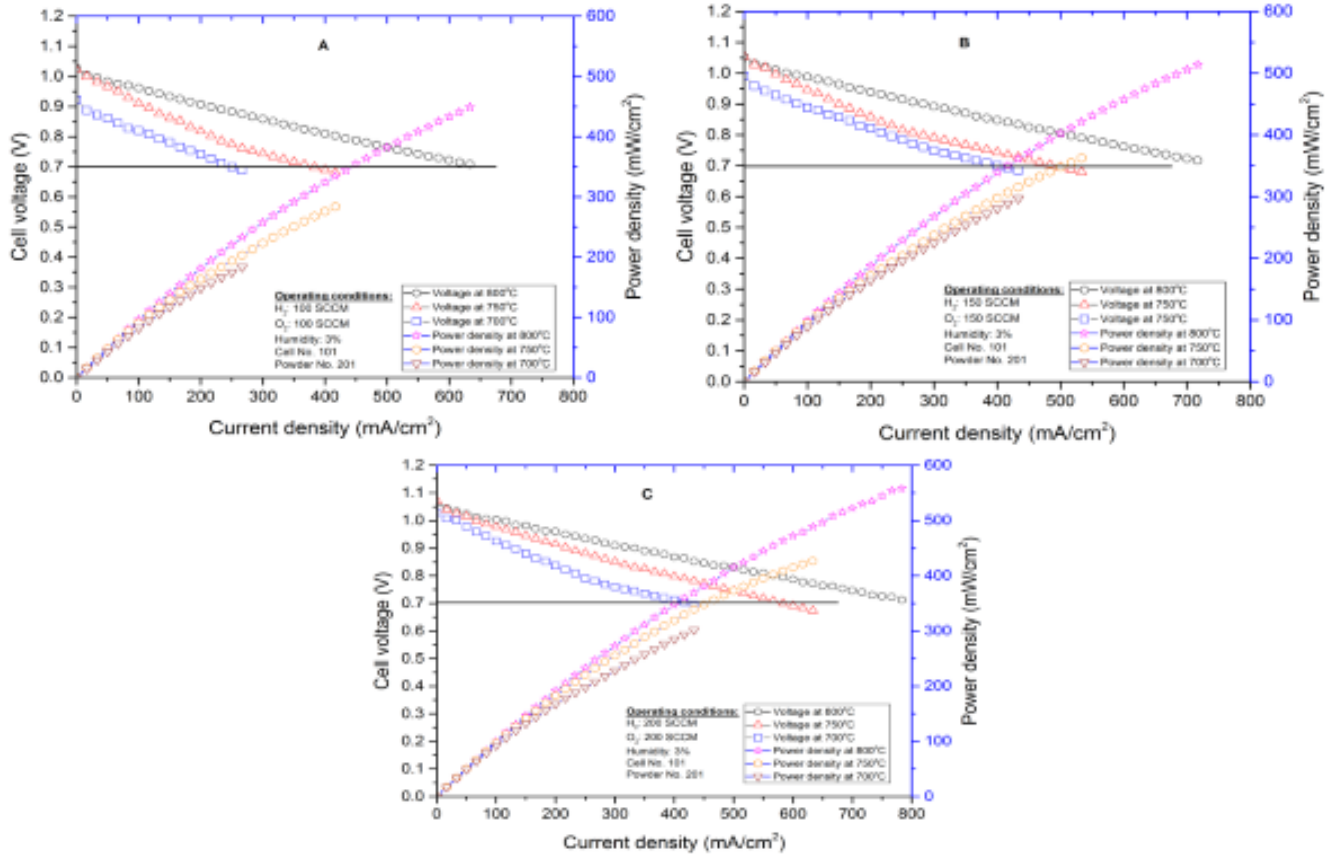


Fig 13 Current –Voltage (I-V) curves and current-power (I-P) curves of an anode supported SOFC single Cell # 101 with different temperatures (700-800°C) and flow rates (100-200sccm)

other authors reported [29]. Table 4 shows the XRD data to determine the average crystallite size of LSM-1 was found to be around 16 nm. It is seen that the milled powder of LSM-1 have little bit smaller crystallite size of 15 nm.

### 3.4. Surface area characterization

Table 5 shows the surface area of the as prepared and calcined LSM powders as respectively. It is seen that the surface area for as prepared powder was  $23.48\text{m}^2/\text{gr}$  and for calcined powder at  $900^\circ\text{C}$   $21\text{ m}^2/\text{gr}$  respectively. The surface area reduced after calcination of LSM-2 nano powder there by increased in particle size as per expectation. The surface area of LM-2 achieved for calcined powder is more than authors reported [32]. It is seen that the approximate average crystalline size calculated from specific surface area  $d_{\text{BET}}$  of the as prepared and calcined LSM powders are 38.65 nm and 48.9 nm respectively assuming the theoretical density of LSM  $6.521\text{ g/cc}$  using the equation [23, 31] and assuming spherical parti-

cles. It can be seen that the average particle size value  $d_{\text{XRD}}$  value is obtained was 15.2 nm from XRD data using Debye Scherrer equation. The  $d_{\text{BET}}$  and  $d_{\text{XRD}}$  values are comparable with other authors reported [32].

### 3.5. Electrochemical characterization of SOFC single Cell

Figures 13a - 13c show the I-V and I-P curves for the single SOFC cell [# 101] with three flow rates 100-200sccm and three operating temperatures 700, 750,  $800^\circ\text{C}$  with  $\text{H}_2\text{-O}_2$  using 3% of humidified hydrogen gas. The OCV values for the cells was approximately 1.08-1.09 V. Such values indicate that a dens structure is well –formed electrolyte on the NiO-YSZ surface so that the leakage is negligible. It is seen from Fig 13a that the maximum current density (cd) obtained is around  $0.63\text{A}/\text{cm}^2$  at a cell voltage of 0.7V and power density (pd) is around  $0.45\text{W}/\text{cm}^2$  at  $800^\circ\text{C}$  with  $\text{H}_2$  and  $\text{O}_2$  flow rates of 100sccm . But, when the cell operating

Table 5. Surface area data and average crystallite size of  $\text{La}_{0.8}\text{Sr}_{0.2}\text{MnO}_3$  (LSM-2) powders

Sample ID Number	Surface Area ( $\text{m}^2/\text{g}$ ) Multipoint BET	Average crystallite size with $d_{\text{BET}} = 6 / [d_{\text{th}} \times S_{\text{BET}}]$ [ 23, 31] nm	Average crystallite size with XRD $d_{\text{XRD}}$ , nm	$d_{\text{BET}}/d_{\text{XRD}}$
201a [LSM-2]	23.48	39.18	---	---
201b [LSM-2]	21.00	43.81	15.20	2.88

$d_{\text{BET}}$  = average crystallite e size,  $d_{\text{th}}$  = theoretical density of LSM ( 6.521 gr/cc),  $S_{\text{BET}}$  = surface area (  $\text{m}^2/\text{gr}$ )

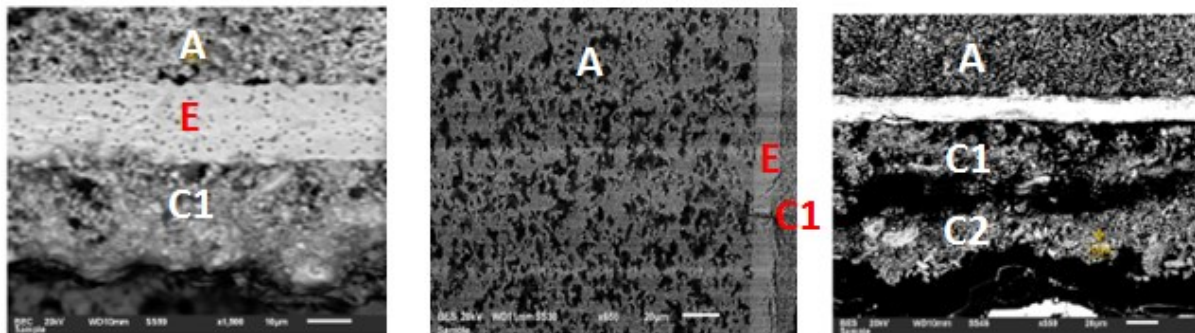


Fig 14 SEM micrographs of Cross section of SOFC Single Cell after testing at 800°C (A : NiO-YSZ, E : Electrolyte, C1 : CFL and C2 : CL- broken during polishing)

temperatures reduced to 750°C and 700°C, the cd and pd values are reduced to 0.42 mA/cm<sup>2</sup> and 0.27A/cm<sup>2</sup> and 0.29 W/cm<sup>2</sup> and 0.20W/cm<sup>2</sup> respectively since the reaction rates reduced due to low temperatures as their ASR values (Table-5) obtained were 0.60-0.70 Ωcm<sup>2</sup> which are higher than accepted values (~less than 0.5 Ωcm<sup>2</sup>) for SOFC application. Figures 13b show the I-V and I-P curves for the single SOFC cell [# 101] with three flow rates 150 sccm and three operating temperatures 700-800°C with H<sub>2</sub>-O<sub>2</sub> with 3% of humidified hydrogen gas. It is seen from Fig 13b that the maximum current density obtained is around 0.72A /cm<sup>2</sup> at a cell voltage of 0.7V and power density is around 0.53W/cm<sup>2</sup> at 800°C with 150 sccm of H<sub>2</sub> and O<sub>2</sub>. It is seen that the cd and pd values increased with increasing gas flow rates to 150 sccm. Similar results observed when the cell operating temperatures reduced to 750°C and 700°C the cd and pd values are reduced to 0.45A/cm<sup>2</sup> and 0.30W/cm<sup>2</sup> respectively.

Figures 13c show the I-V and I-P curves for the single SOFC cell [# 101] with the flow rates 200 sccm and three operating temperatures 700-800°C with H<sub>2</sub>-O<sub>2</sub> with 3% of humidified hydrogen gas. It is seen from Fig 13c that the maximum current density obtained is around 0.80A /cm<sup>2</sup> at a cell voltage of 0.7V and power density is around 0.55W/cm<sup>2</sup> at 800°C. But, when the cell operating temperatures reduced to 750°C and 700°C, the cd and pd values are reduced to 0.43A/cm<sup>2</sup> and 0.3W/cm<sup>2</sup>. Although at lower temperatures (700-750°C) the cd and pd values are low due to several reasons like YSZ content in the CFL, its thickness more than planned (~18 microns) as it was screen printed manually. It is observed that the cd and pd values obtained were 0.80A/cm<sup>2</sup> and 0.55W/cm<sup>2</sup> at the gas flow rates of 200sccm and operating temperature 800°C with the

LSM-2 as CL and LSM-1 with 50%YSZ as CFL over the YSZ electrolyte. It is depicted that here is no much appreciable power output by raising fuel flow rates to 200sccm. These results obtained in the present work are in agreement with other researchers reported [26,34]. There may be several reasons for lowering the current density and power density like starvation of fuel and lowering reaction kinetics at the cathodes specially at low temperatures of 700-750°C. So it is planned to develop special cathode materials like CGO / LSCF and with different anode functional layers to obtain higher output power at lower temperatures ~700°C as reported by Moon et al [34]. Table 5 shows the area surface resistance (ASR) values obtained (0.40-0.5Ωcm<sup>2</sup>) at 0.7V, 800°C these are quite comparable and agreement with other authors reported elsewhere [34,35]. So such cells can be used with combination of LSM-1 and LSM-2 as cathode materials for low temperature (800°C) SOFCs application. The parameters of the anode side that affect the single cell performance are its microstructure, pore / pore size distribution, three phase boundary, anode electrolyte interference, anode thickness etc. These parameters which result in the voltage loss of cells at a given operating current density, include concentration / activation polarization of electrode and Ohmic polarization of anode/electrolyte interferences.

Figures 14a -14c show the cross section of the SOFC single cell showing the different layers of CFL and CL, YSZ and NiO-YSZ. The YSZ electrolyte with 13 microns supported by the anode with 1.5mm in thickness. The YSZ layer was essentially dense, uniform with no open pin holes. It had continuous and crack free surface morphology. It is seen that both the anode and cathode layer were well-adhered to the electrolyte layer. It is also seen that the thick-

Table 6. Area specific resistance (ASR) at different flow gas rates, temperatures, current density and power density values

Flow rates of H <sub>2</sub> and O <sub>2</sub> (sccm)	Operating temperatures (°C)	Current density mA/cm <sup>2</sup> at 0.7V	Max. power density W/cm <sup>2</sup>	Area specific resistance (Ω.cm <sup>2</sup> )
100	700	0.27	0.20	0.799
	750	0.42	0.29	0.655
	800	0.63	0.45	0.474
150	700	0.45	0.34	0.694
	750	0.53	0.35	0.582
	800	0.75	0.53	0.446
200	700	0.43	0.30	0.617
	750	0.60	0.43	0.553
	800	0.80	0.55	0.428

ness of CFL and CL are little bit more which may also contributed for lowering the power output specially at lower temperature of cell operation specially as the resistance increases with increasing the thickness of the layers. By reducing the %YSZ in CFL layer, lowering CL layer thickness and introducing anode functional layer as studied by moon et al [33] may yield better performance of the SOFC cells. The work is in progress on these lines.

#### 4. CONCLUSIONS

The following conclusions are drawn from the present work:

1. The LSM -1 and LSM-2 nanoceramic cathode powders were prepared using auto-ignition technique with c/n: 0.50 with average crystallite size of 15-16 nm
2. SEM images indicate Particle size of the LSM powders indicate less than 300nm.
3. TGA plots for LSM as prepared powders indicate that there is no weight change after 600°C which indicates the completing of combustion.
4. XRD patterns shows the formation of pure LSM powders after calcination of the ash obtained with auto- ignition at 900°C/ 4hrs
5. Cathode functional layer (CFL) with 50% YSZ worked satisfactory achieved reasonable current density and power density. However, by reducing further the % of YSZ in CFL may yield higher current density and power density
6. The surface area of the LSM-2 powder was found to be 23.4 m<sup>2</sup>/gr and 21 m<sup>2</sup>/g for as prepared and sintered powders respectively.
7. The current density and power density values obtained are 0.80A/cm<sup>2</sup> at 0.7V and 0.55W/cm<sup>2</sup> respectively at 800°C cell operating temperature with H<sub>2</sub> and O<sub>2</sub> with 150 sccm. There is no appreciable increase in cd and pd using higher hydrogen and oxygen flow rates of 200sccm.
8. The Area surface resistance (ASR) values obtained were in the range of 0.40 - 0.5Ωcm<sup>2</sup> at 0.7 V at 800°C.

#### 5. FUTURE WORK

To study with different YSZ contents (30-70%) in cathode functional layer (CFL) and different anode function layers on electrochemical characteristics and study the particle size distribution in LSM nano ceramic powders.

#### 6. ACKNOWLEDGEMENTS

Authors would like to thank Dr.Omar A. Alharbi, Research Professor at WERI, KACST, Riyadh for providing XRD patterns of LSM powders. Also authors are thankful to the Fuel cell team members for their assistance during the experimental work, preparing the nano ceramic powders and SOFC cell testing.

#### REFERENCES

- [1] Liu M L, Lynch M E, Blinn K, Alamgir F M,Choi Y. Mater Today, 14, 534 (2011).
- [2] Yang L, Choi Y, Qin W T, Chen H Y, Blinn K, Liu M L., Science, 326, 126 (2009).
- [3] Huang Y H, Dass R I, Xing Z L., Goodenough JB., Science,

- 3121, 254 (2006).
- [4] S.C. Singhal , K. Kendell, Elsevier, Oxford, UK Editor, (2003).
- [5] T.-L. Wen., D. Wang , M. Chen, H.Z.Zhang , H.Nie, W.Huang, Solid State Ionics, 148, 513 (2002).
- [6] <http://www.springer.com/978-1-4614-1956-3>, and Chendong Zuo, Mingfei Liu and Meilin Liu-2<sup>nd</sup> Chapter - Solid Oxide Fuel Cells, M.Aparicio et al (eds), Sol-Gel processing for Conventional & Alternative Energy, Advances in Sol-Gel Derived Materials and Technologies, 2012.
- [7] Gaudon M, Laberty-Robert C, AnsartF,Steven P, Rousset A, Solid State Science, 4(1), 125 (2002).
- [8] M. Ghouse, Y.M. Alyousef , A. Al Musa, M.F. Alotaibi, Int. J. Hydrogen Energy, 35, 9411 (2010).
- [9] J.H Huo, H.Uanderson, Solid State Chemistry, 87, 55 (1990).
- [10]Ze Liu, MingfeiLiu,Lei Yang, Mielin Liu, Journal of Energy Chemistry, 22, 555 (2013).
- [11]Sakai N, Kawada T, Yokokawa H, Dokia M, Iwata T, Mater. Science, 25, 4531 (1990).
- [12]P. Decorse, G. Caboche, L.-C.Dufour, Solid State Ionics, 117, 161 (1991).
- [13]Singhal S C, Solid State Ionics, 152, 405 (2002).
- [14]Jiang S P, Solid State Ionics, 146, 1 (2002).
- [15]P. Pal, M.W. Raja, J. Mukhopadhyay, A. Dutta, S. Mahanty, R.N. Basuand, H.S. Maiti, ECS Transactions, 7(1), 1129 (2007).
- [16]V.A.H. Haanapple, D. Rutenbeck, A. Mai, S. Uhlenbruck, D. Sebold, H. Wesemeyer, B. Rowekamp, C. Tropartz, F. Tietz, Journal of Power Sources, 130, 119 (2004).
- [17]H.P. Buchkremer, U. Dieckmann, D. Stover, Proceedings of the Second European Solid Oxide Fuel Cell Forum, Oslo, Ulf Bossel, May, 1996, p.221.
- [18]R.N. Basu, S.K. Pratihari, M.Saha,H.S.Maiti, "preparation of Sr-sustitute LaMnO<sub>3</sub> thick films as cathode for solid oxide fuel cell , Materials Letters, 32 (1997) 217-222.
- [19]A. Chakrborthy, P.S. Devi and H.S. Maiti, J. Mater. Res., 10, 918 (1995), and A. Chakraborty, R.N. Basu, M.K. Paria, H.S. Maiti, Proc. the 4<sup>th</sup> Inter. Sym.on Solid Oxide Fuel Cell, Yokohoma, Japan, June, 18-23, 1995.
- [20]Y.M. Alyousef, F.S. Alenazey, M. Ghouse, G.N. Almutairi and A.E. Aldossary, International Journal of Engineering and Innovative Technology ( IJEIT), 3, 26 (2014).
- [21]<http://www.tosoh.com/our-products/advanced-materials/zirconia-powders>
- [22]B.D. Cullity, 2<sup>nd</sup>Edn Addison-Wesly publication Co.Inc, Reading, Massachussts, USA,(1978), p.102.
- [23]J. Jung, L. Gao, Journal of Solid State Cghemistry, 177 1425 (2004).
- [24]R.N. Basu, A. Das Sharma, A. Dutta and J. Mukhopadhyay, International Journal of Hydrogen Energy, 33, 20, 5748 (2008).
- [25]R.N. Basu, A. Das Sharma, A. Dutta and J. Mukhopadhyay, H.S. Maiti, The Electrochemical Society, 7, 1, 227 (2007).
- [26]Sun-Dong Kim, Hwan Moon, Sang-Hoon Hyun, Jooho Moon, Joosun Kim, Hae-Weon Lee, Solid State Ionics, 177, 931

- (2006).
- [27]Jung-Hoon Song, Sun-II Park, Jong H.O. Lee, H.O-Sung Kim, Journal of Materials Processing Technology, 198, 414 (2008).
- [28]J.X. Wang, Y.K. Tao, J. Shao, W.G. Wang, Journal of Power Sources, 186, 344 (2009).
- [29]A. Dutta, J. Mukhopadyaay, R,N. Basu, Journal of the European Ceramic Society, 29, 2003 (2009).
- [30]L.M.P. Garcia, D.A. Macedo, G.L. Souza, F.V. Motta, C.A. Paskocimas R.M. Nascimento, Cramics International, 2014.
- [31]S. Ghosh, S. Dasgupta, Materials Science-Poland, 28, 421 (2010).
- [32][www.intechopen.com/http://cdn.intechopen.com/pdfs-wm/36185.pdf-page392](http://www.intechopen.com/http://cdn.intechopen.com/pdfs-wm/36185.pdf-page392).
- [33]R. Moriche, D. Marrero-Lopez, F.J. Gotor, M.J. Sayagues, Journal of Power Sources, 252, 43 (2014).
- [34]H. Moon, S.D. Kim, S.H. Hyun, H.S. Kim, Journal of Hydrogen Energy, 33, 1758 (2008).
- [35]S.D. Kim, S.H. Hyun, J. Moon, J.H. Kim, Rak Hyun Song, J. of Power Sources, 139, 67 (2005).